



Particulate matter constituents trigger the formation of extracellular amyloid β and Tau - containing plaques and neurite shortening *in vitro*

Aleksandar Sebastijanović, Laura Maria Azzurra Camassa, Vilhelm Malmborg, Slavko Kralj, Joakim Pagels, Ulla Vogel, Shan Zienolddiny-Narui, Iztok Urbančič, Tilen Koklič & Janez Štrancar

To cite this article: Aleksandar Sebastijanović, Laura Maria Azzurra Camassa, Vilhelm Malmborg, Slavko Kralj, Joakim Pagels, Ulla Vogel, Shan Zienolddiny-Narui, Iztok Urbančič, Tilen Koklič & Janez Štrancar (2024) Particulate matter constituents trigger the formation of extracellular amyloid β and Tau -containing plaques and neurite shortening *in vitro*, *Nanotoxicology*, 18:4, 335-353, DOI: [10.1080/17435390.2024.2362367](https://doi.org/10.1080/17435390.2024.2362367)

To link to this article: <https://doi.org/10.1080/17435390.2024.2362367>



© 2024 The Author(s). Published by Informa UK Limited, trading as Taylor & Francis Group



[View supplementary material](#)



Published online: 22 Jun 2024.



[Submit your article to this journal](#)



Article views: 914













[View related articles](#)



[View Crossmark data](#)

Particulate matter constituents trigger the formation of extracellular amyloid β and Tau -containing plaques and neurite shortening *in vitro*

Aleksandar Sebastijanović^{a,b} , Laura Maria Azzurra Camassa^c , Vilhelm Malmborg^{d,e,f} , Slavko Kralj^g , Joakim Pagels^{e,f} , Ulla Vogel^d , Shan Zienolddiny-Narui^c , Iztok Urbančič^b , Tilen Koklič^b  and Janez Štrancar^{a,b} 

^aInfinite LLC, Maribor, Slovenia; ^bLaboratory of Biophysics, Condensed Matter Physics Department, Jožef Stefan Institute, Ljubljana, Slovenia; ^cNational Institute of Occupational Health, Oslo, Norway; ^dNational Research Centre for the Working Environment, Copenhagen, Denmark; ^eErgonomics and Aerosol Technology, Lund University, Lund, Sweden; ^fNanoLund, Lund University, Lund, Sweden; ^gMaterial Synthesis Department, Jožef Stefan Institute, Slovenia

ABSTRACT

Air pollution is an environmental factor associated with an increased risk of neurodegenerative diseases, such as Alzheimer's and Parkinson's, characterized by decreased cognitive abilities and memory. The limited models of sporadic Alzheimer's disease fail to replicate all pathological hallmarks of the disease, making it challenging to uncover potential environmental causes. Environmentally driven models of Alzheimer's disease are thus timely and necessary. We used live-cell confocal fluorescent imaging combined with high-resolution stimulated emission depletion (STED) microscopy to follow the response of retinoic acid-differentiated human neuroblastoma SH-SY5Y cells to nanomaterial exposure. Here, we report that exposure of the cells to some particulate matter constituents reproduces a neurodegenerative phenotype, including extracellular amyloid beta-containing plaques and decreased neurite length. Consistent with the existing *in vivo* research, we observed detrimental effects, specifically a substantial reduction in neurite length and formation of amyloid beta plaques, after exposure to iron oxide and diesel exhaust particles. Conversely, after exposure to engineered cerium oxide nanoparticles, the lengths of neurites were maintained, and almost no extracellular amyloid beta plaques were formed. Although the exact mechanism behind this effect remains to be explained, the retinoic acid differentiated SH-SY5Y cell *in vitro* model could serve as an alternative, environmentally driven model of neurodegenerative diseases, including Alzheimer's disease.

ARTICLE HISTORY

Received 26 December 2023
Revised 25 April 2024
Accepted 27 May 2024

KEYWORDS






Neurite shortening; neuronal degeneration; amyloid β (A β); microtubule-associated protein (Tau); air pollution; particulate matter constituents; TiO₂ nanotubes; diesel exhaust; CeO₂ nanoparticles; iron oxide


1. Introduction

1.1. Particulate matter in polluted air is associated with cognitive decline and Alzheimer's disease, yet causality is still not fully established

Strong correlations between particulate air pollution and dementia suggest airborne particulate matter as a possible environmental trigger of neurodegenerative diseases (Peeples 2020; Shi et al. 2020, 2021). However, whether the particulate matter in air pollution can cause dementia remains controversial (Underwood 2017). It is well-established that high levels of air pollution, particularly particulate matter smaller than 2.5 μm (PM_{2.5}), are associated with cognitive decline and Alzheimer's disease (AD) (Carey et al. 2018; Younan et al. 2020; Zhang, Chen,

and Zhang 2018). However, it is important to note that the strength of this association does not necessarily imply causation. How air pollution particles enter the brain and possibly trigger neurodegeneration remains an open question (Underwood 2017). Nevertheless, a recent study has observed epigenetic gene regulation changes that are typically found in Alzheimer's patients in both young adults and mice exposed to particulate air pollution (Calderón-Garcidueñas et al. 2020). In another study, the authors indicate that there may be no safe exposure limit to outdoor fine particulate air pollution (PM_{2.5}) in relation to the risk of dementia (Weichenthal et al. 2022). Considering the emerging evidence, the Lancet Commission recognized air pollution as a risk factor for dementia, suggesting

CONTACT Janez Štrancar  janez.strancar@infinite-biotech.com  Infinite Biotech LCC, Maribor, Slovenia; Tilen Koklič  tilen.koklic@ijs.si; Iztok Urbančič  iztok.urbancic@ijs.si  Laboratory of Biophysics, Condensed Matter Physics Department, Jožef Stefan Institute, Ljubljana, Slovenia

 Supplemental data for this article can be accessed online at <https://doi.org/10.1080/17435390.2024.2362367>.

© 2024 The Author(s). Published by Informa UK Limited, trading as Taylor & Francis Group
This is an Open Access article distributed under the terms of the Creative Commons Attribution-NonCommercial-NoDerivatives License (<http://creativecommons.org/licenses/by-nc-nd/4.0/>), which permits non-commercial re-use, distribution, and reproduction in any medium, provided the original work is properly cited, and is not altered, transformed, or built upon in any way. The terms on which this article has been published allow the posting of the Accepted Manuscript in a repository by the author(s) or with their consent.

that reducing air pollution could potentially prevent or delay the onset of dementia, which is vital because pre-symptomatic diagnosis of disease is still lacking (Livingston et al. 2020).

AD, in particular, is a most prevalent form of dementia characterized by early memory loss and progressive damage to brain cells in the hippocampus, a region responsible for learning and memory (Drew 2018). Despite more than half a century of research, the exact causes of the disease remain uncertain, and no effective treatment yet exists (Drew 2018), despite recently FDA-approved therapies (Couzin-Frankel 2023; Piller 2023). Neurodegenerative diseases, such as AD, Parkinson's, amyotrophic lateral sclerosis, and Huntington's disease, are characterized by the misfolding and aggregation of specific proteins into large plaques (Eftekharzadeh, Hyman, and Wegmann 2016). Epidemiological data suggest that nanoparticles accumulated in the brain might trigger the formation of AD-like plaques. Furthermore, imaging of thin sections of amyloid cores from AD patients has corroborated the presence of ambient magnetite nanoparticles in the plaques (Plascencia-Villa et al. 2016). Although, most studies linking ambient air pollution with neurodegenerative disease have considered PM_{2.5} as an exposure metric, ultrafine particles (PM_{0.1}) or nanoparticles (NP) are even more numerous, cause more inflammation, and can translocate to essentially all organs (Schraufnagel 2020). It has been suggested that combustion emissions such as diesel exhaust particles and engineered nanoparticles are of special importance in neurodegenerative disease (Calderón-Garcidueñas and Ayala 2022). Existing research thus shows the need for new methods to confirm the causal connection between the components of particulate matter and neurodegeneration.

Based on a recent systematic review of literature focusing on organic environmental pollutants, Lopez-Suarez et al. proposed the SH-SY5Y cell line for neurotoxicity research. Namely, the effects on cultured SH-SY5Y cells include autophagy, several types of cell death, increased oxidative stress, mitochondrial dysfunction, neurotransmitter homeostasis disruption, and neuritic shortening (Lopez-Suarez et al. 2022), which are all subcellular/cellular hallmarks of neurodegenerative diseases (NDD) (Wilson et al. 2023). The SH-SY5Y cell line is a popular model for Parkinson's disease (PD) as it possesses many characteristics of dopaminergic neurons (Xie, Hu, and Li 2010). The dopaminergic system is also involved in the progression (Martorana and Koch

2014), and especially in the early stages of AD (Sala et al., 2021). For example, degeneration of dopaminergic neurons in the ventral tegmental area at pre-plaque stages leads to memory dysfunction (Nobili et al. 2017). Although amyloid plaques, deposits of the β -amyloid (A β) peptide (Glennner and Wong 1984), are defining lesions in the Alzheimer's disease (AD) brain.

Therefore we hypothesize that the retinoic acid-differentiated SH-SY5Y cells are potentially a relevant model for late-onset (sporadic) AD, which is more prevalent (>95%) than the early-onset (familial) variant (Masters et al. 2015). Whereas there are models for the familial type of AD, such as transgenic 5XFAD mice that rapidly accumulate massive cerebral A β 42 levels, resembling Alzheimer's disease amyloid plaque formation (Oakley et al. 2006), the models for late-onset AD that wouldn't form amyloid beta plaques spontaneously are still sparse or incomplete. Here we show that retinoic acid-differentiated SH-SY5Y cells do not spontaneously form amyloid beta plaques (Riegerová et al. 2021). Therefore, the differentiation process is insufficient to cause the formation of amyloid beta plaques. Instead, other studies often introduce amyloid-beta peptides externally in order to induce plaque formation in a non-genetically modified model that doesn't produce them spontaneously (He et al. 2018).

In this paper, we investigated whether exposure of neuron-like cells to particulate matter constituents could replicate neurodegenerative phenotypes *in vitro*. These include the formation of extracellular amyloid- β -containing plaques and reductions in both neurite density and length. Employing a high dose *in vitro* exposure of neurons allowed us to emulate a dose accumulated over a lifetime, delivering it within approximately a day, depending on the sedimentation rate of the nanomaterial. Previously, we employed a similar high-dose *in vitro* exposure technique in a coculture of lung epithelial cells and alveolar macrophages, successfully replicating phenotypic characteristics observed in long-term lung inflammation occurring 90 days after exposure in mice (Danielsen et al. 2020; Kokot et al. 2020).

We tested four types of nanomaterials: two engineered nanomaterials and two nanomaterials commonly found in polluted air:

1. **anatase TiO₂ nanotubes** are an engineered nanomaterial relevant predominantly to occupational risk. In general, TiO₂, regardless of

its form and crystalline structure, also known as E171, is widely used as a white colorant in food, paints, coatings, pharmaceuticals, cosmetics, and even toothpaste. E171 contains a fraction of nanosized primary particles (<100 nm) (Peters et al. 2014, 2020). Several *in vivo* studies reviewed by Song et al. (Song et al. 2015) have demonstrated that the TiO₂ nanoparticles can be transported and accumulated in the brain, but mostly in intranasal instillation or inhalation studies, via a nose-to-brain path, eventually leading to central nervous system dysfunctions. Another group showed that titanium content in mouse hippocampus after 90 days of continuous intranasal exposure to TiO₂ nanoparticles was 0.6 mg/g tissue at the highest administered dose of 10 mg/kg body weight (Ze et al. 2014), much higher than the levels observed in humans. In the case of engineered nanoparticles, functionalization with KD8 peptide has been used to enhance their ability to cross the blood-brain barrier and accumulate at the site of Aβ deposits in the brain. Thus, for such purposefully engineered nanoparticles, ingestion or intra-venous injection with subsequent delivery across the blood-brain barrier might also be important (Haochen Zhang et al., 2022). Titanium can be found in human tissue at lower average concentrations ranging from 1 μg/g (Peters et al. 2020) up to 80 μg/g (Baj et al. 2023) in the human brain. Thus, neuroinflammation and spatial memory impairment observed in mice occur at more than ten times higher brain content than in humans. The effect of TiO₂ nanoparticles on the brain is thus still controversial since detrimental effects are observed only at very high doses. Here, we also use a very high concentration of 3 mg/g (mass of a nanomaterial (mg) versus mass of cells (g), supplement page 40), akin to *in vivo* dosages, to show that inflammatory, engineered TiO₂ nanotubes induce the formation of extracellular amyloid β-containing plaques and cause shortening of neurites. Yet, they do not cause such extensive neurite shortening as iron oxide and diesel exhaust particles.

2. **Iron oxide (γ-Fe₂O₃) nanoparticles** are commonly found in road traffic emissions from brake wear (Maher 2019). Metal ions such as copper, iron, and zinc have been found in

Alzheimer's disease senile plaques. Copper, in particular, binds to beta-amyloid peptides with high affinity, promotes Aβ aggregation, and contributes to neurotoxic reactive oxygen species formation (Du et al. 2021). Postmortem analyses of amyloid plaques revealed copper, iron, and zinc accumulation by 5.7, 2.8, and 3.1 times the levels observed in normal brains, respectively (Liu et al. 2019). However, the origin of metal ions in Alzheimer's disease plaques is not understood. Our extensive review of the current literature yielded no references regarding the possible environmental origin of metal oxides. On the other hand, there is plenty of evidence that polluted air from coal combustion contains several metals, including iron (Suarez and Ondov 2002). The PM_{2.5} concentrations of iron oxide particles is high in underground railway stations. Sheikh et al. (Sheikh et al. 2022) showed that the majority of iron oxide particulate matter exposure in the London Underground was maghemite, the material used in our study, as confirmed by Mössbauer analyses (Tadic et al. 2014). Occupational exposure to welding fume particles (iron-rich particles and magnetite) is associated with an increased risk of developing AD. Finnegan et al. showed that non-chemically preserved AD patients' postmortem tissue samples contained the average concentration of iron peaking at 400 mg/g (Finnegan et al. 2019). Furthermore, airborne iron oxide (magnetite) particles can be concentrated in smaller regions of the human brain (Maher et al. 2016), thus reaching even higher local concentrations. Such magnetite nanospheres are ubiquitous and abundant in airborne particulate matter pollution. They are smaller than 200 nm in diameter and can enter the brain directly via the olfactory bulb (Maher et al. 2016). Examination of the human frontal cortex brain samples obtained from subjects who lived in Mexico City revealed that magnetite nanoparticles have an external, rather than an endogenous source (Maher et al. 2016). Although the highest brain magnetite concentration was 10 μg/g of dry tissue, the transmission electron micrographs of brain thin sections showed that the nanoparticles are in about 1% of the total area; thus *in vitro* concentrations of 1 mg/g might be more relevant to human exposure to polluted air.

3. Since iron is present in most **diesel exhaust** samples, representing on average about 20% w/w (Viskup, Wolf, and Baumgartner 2020), we estimate that the brain burden of diesel exhaust particles might reach up to 2 mg/g tissue weight, coinciding with the dosage used in this manuscript. Although iron might not be a good exposure metric for diesel exhaust, we also considered an exposure concentration of 100 $\mu\text{g}/\text{m}^3$ as elemental carbon (Debia et al. 2017), to estimate the exposure over an entire working life (Supplement Chapter 7 Dose relevance). The specific surface area of diesel exhaust particles is similar to particles generated by welding, with particle sizes mostly below 200 nm, so the concentration of insoluble surface area that might accumulate in the brain may be in the same range as occupational exposure of welding workers, given that the transport mechanisms across barriers are similar for the two types of aerosols.
4. As an example of reportedly nontoxic particulate matter, we tested **CeO₂ nanoparticles**, which are used as fuel additive in motor vehicles to reduce carbon monoxide, nitrogen oxides, and hydrocarbons in exhaust gases. Thus, the particles are released into the air. The effects of CeO₂ nanoparticles reported in the literature are contradictory, demonstrating all kinds of effects, from protective to toxic (Gagnon and Fromm 2015). For example, CeO₂ nanospheres and nanorods improved cognitive impairment following mild traumatic brain injury in VC57BL/6J male mice at the dose of 0.02 mg/g body weight. However, the concentration in the brain was not reported (Fiorani et al. 2015; Gagnon and Fromm 2015).

1.2. The challenge of reproducing all hallmarks of Alzheimer's disease (AD) in animal models: the limitations of genetically modified models and the need for an environmentally triggered model

AD is defined by a triad of pathological hallmarks (1) amyloid β peptide plaques, (2) aggregation of Tau protein, and (3) neuronal degeneration. Accumulation of amyloid β plaques precedes cognitive impairment by at least 20 years (Scheltens et al. 2016). Extracellular deposits of amyloid β have long been considered the initial event of the disease process (Leng and Edison 2021), at least in less

prevalent familial cases (Karran, Mercken, and Strooper 2011). The accumulation of Tau into large aggregates, initially appearing in dystrophic neurites surrounding A β plaques, is usually referred to as neuritic plaque tau (NP tau, followed by the formation and spread of neurofibrillary tangles (NFT) and neuropil threads to other neurons. Recently He et al. presented a new mouse model, which offered a new way to explain how the amyloid β plaque environment accelerates the spread of Tau pathology in AD patients' brains, consistent with imaging studies and investigations of postmortem AD brains (He et al. 2018). Axonal and dendritic degeneration and neuronal death, reflected in reduced neuronal arborization and decreased neuron density, is the final pathological hallmark that coincides with the appearance of intracellular Tau deposits and symptoms of advanced cognitive decline (Falke et al. 2003).

Here, we show that high-dose *in vitro* exposure of neurons to particulate matter constituents, such as diesel exhaust and iron oxide nanoparticles, replicates hallmarks of AD pathology by triggering amyloid β plaque formation and reducing the density and length of neurites. Since less than 0.1% (Blennow, de Leon, and Zetterberg 2006) of AD is caused by a single genetic mutation, the model system consisting of neurons without familial mutations might thus be regarded as an alternative, perhaps more relevant, environmentally driven model of neurodegenerative diseases, including Alzheimer's disease.

2. Materials and methods

2.1. Cell line

The cells we refer to as neurons throughout the manuscript are retinoic acid (RA) differentiated human neuroblastoma SH-SY5Y cell line. The undifferentiated SH-SY5Y human neuroblastoma cell line is commercially available from the American Type Culture Collection (ATCC, www.atcc.org or www.lgcstandardsatcc.org, catalog number CRL-2266™). The SH-SY5Y is a comparatively homogeneous human neuroblastoma cell line (ATCC® CRL-2266™) is one of the neurosciences' most used cell lines, either undifferentiated or differentiated into neuron-like cells. The SH-SY5Y cell line exhibits several neuronal markers when differentiated with retinoic acid (RA) to a more mature neuron-like phenotype (Kovalevich and Langford 2013). Differentiation with RA results in the cells becoming

more polarized, extending long neurites, and forming functional synapses (Martin, Gandawijaya, and Oguro-Ando 2022). Besides, as they are human-derived, SH-SY5Y neuroblastoma cells express several human-specific proteins that are missing in rodent primary cultures or animal models. The cells grew as a mixture of floating and adherent cells in DMEM/F-12 (Gibco) medium supplemented with 1% penicillin/streptomycin (Sigma-Aldrich), 2 mM GlutaMax (Gibco), and 10% FBS (BioChrom AG). For SH-SY5Y differentiation, we seeded 1×10^6 cells cm^{-2} on the collagen-coated, microscopy-adapted plates (8-wells, Ibidi). After 24 hours we added the differentiation medium containing Dulbecco's modified eagle medium DMEM/F12 without phenol red (#21041025, Thermo Fisher), supplemented with 1% penicillin/streptomycin (Sigma-Aldrich), 2 mM GlutaMax (Gibco), 0.5% FBS (BioChrom AG) and 10 μM retinoic acid (fisher scientific, #AC207341000). Old media was replaced with 100 μL fresh differentiation media every other day, until 7th day when we terminated the differentiation.

2.2. Nanomaterial preparation

We employed a dispersion technique using cup horn sonication to disperse materials, namely anatase TiO_2 , maghemite $\gamma\text{-Fe}_2\text{O}_3$, CeO_2 , and diesel exhaust particles, in a buffer. The buffer solution utilized in this study was 1 mM bicarbonate buffer with a pH of 10, which was specifically chosen due to its low osmolarity and high pH properties that minimize the charge screening of the active surface of the materials.

To ensure uniform dispersion of the materials in the bicarbonate buffer, the materials were resuspended so that each 3 μL of the suspension contained 3 cm^2 of the material surface. The weighted mass of each material and the volumes of bicarbonate buffer utilized to prepare the solutions are presented in the Table 1.

The synthesis of TiO_2 nanotubes followed a rigorous procedure and has been extensively documented (Umek et al. 2007). In brief, the process began with the controlled hydrothermal synthesis of sodium titanate nanotubes. These sodium titanate nanotubes were subsequently subjected to ion exchange to transform them into hydrogen titanate nanotubes. Finally, through a carefully conducted thermal treatment, the hydrogen titanate nanotubes were successfully converted into the desired TiO_2 nanotubes. The detailed methodology and

experimental conditions can be found in the comprehensive study by Umek et al. (2007).

The iron oxide nanoparticles in the form of maghemite ($\gamma\text{-Fe}_2\text{O}_3$) were synthesized by co-precipitation from aqueous solutions of Fe^{2+} and Fe^{3+} salts. The synthesis methodology is described in detail in our previous publications (Kralj et al. 2012; Kralj and Makovec 2014; Nemeč et al. 2020). The saturation magnetization of as-synthesized nanoparticles is $\sim 64 \text{ emu g}^{-1}$. The size of nanoparticles was $11.6 \pm 2.1 \text{ nm}$ which was estimated by analyzing 100 transmission electron microscopy images using ImageJ software. For the preparation of stable colloidal suspension of superparamagnetic nanoparticles its surface was electrostatically stabilized using citric acid as described elsewhere (Nemeč and Kralj 2021). The final concentration of citric-acid stabilized iron oxide maghemite nanoparticles in aqueous suspension was 1.8 mg mL^{-1} .

DEP9.7 diesel exhaust particles were collected after treatment from an experimental modern heavy-duty diesel engine under highly controlled combustion conditions in a laboratory environment. The particle production and collection have been described in detail previously (Gren et al. 2020). The engine was operated to control the physical and chemical properties of the diesel exhaust particles (DEP9.7). To produce the DEP9.7 particles, the engine was run at an engine intake O_2 concentration of 9.7% using petroleum-based ultralow-sulfur diesel fuel of Swedish MK1 standard. The diesel engine combustion was modified to this low-temperature combustion condition using a high amount of exhaust gas recirculation. The exhaust gas recirculation lowers flame temperatures and reduces both soot formation and soot oxidation processes. Using the high control of the engine, the DEP9.7 particles were intentionally designed to have a high content of polycyclic aromatic hydrocarbons (PAH) and refractory organic carbon relative to the content of elemental carbon. DEP9.7 has been characterized extensively (Bendtsen et al. 2020, p. 6; Gren et al. 2020). DEP were collected on a Teflon filter and extracted using methanol with $>80\%$

Table 1. Preparation of nanomaterial dispersions used in this study.

Material	Mass (mg)	Volume (mL)	BET ($\text{m}^2 \text{g}^{-1}$)	Final concentration (mg mL^{-1})
TiO_2 nanotubes	1.0	1.6	150	0.65
$\gamma\text{-Fe}_2\text{O}_3$	1.80	1.0	109	1.80
CeO_2	1.6	1.0	65	1.60
Diesel exhaust particles (DEP9.7)	1.0	2.0	152	0.50

recovery. The DEP9.7 had a primary particle size of 22 nm and an estimated specific surface area of $152\text{ m}^2\text{ g}^{-1}$. The carbon content in DEP9.7 is 33% elemental carbon and 67% organic carbon of which 33% is refractory organic carbon. DEP9.7 contains a number of metals (Bendtsen et al. 2020, p. 6) predominately Cu ($2349\ \mu\text{g g}^{-1}$), Fe ($220\ \mu\text{g g}^{-1}$), Sr ($99\ \mu\text{g g}^{-1}$) and Mn ($92\ \mu\text{g g}^{-1}$). DEP9.7 has a high content of PAH (26.8 mg g^{-1}) and a list of specific PAH can be found in (Bendtsen et al. 2020, p. 6). In comparison to four other sample types from the same engine, DEP9.7 had the lowest formation of Reactive Oxygen Species in the cell free DCFH assay on a mass basis. Extractable organic matter from DEP9.7 had the highest genotoxicity potential in lung epithelial (A549) cells of the five samples (Rothmann et al. 2023).

CeO₂ NPs '50nm agglomerates' composed of 5 nm CeO₂ nanoparticles as determined from TEM images (batch AN-123) were produced and characterized by Applied NanoParticles - A Nanotech Engineering Company (Spain) (<https://www.appliednanoparticles.eu/>). CeO₂ NPs have a mean diameter of $6.2 \pm 1.3\text{ nm}$ as measured by TEM, the agglomerates have a mean diameter of $200 \pm 6\text{ nm}$ as measured by DLS and a zeta potential $-32.5 \pm 0.07\text{ mV}$ measured in miliQ water at pH 9 at 0.5 mS cm^{-1} .

The resulting suspensions of the nanomaterials were then subjected to cup horn sonication in an ice bath for 15 min, utilizing 5 seconds on – 5 seconds off regime for a total duration of 30 min, at a power setting of 20–30W (amplitude 70) to guarantee optimal dispersion.

The volume of material dispersion containing a 10 times larger surface than that of neurons was added in a dropwise manner, prior to microscopy, to cover the surface of the *in vitro* model. The volume applied to cells never exceeded 10% of the media volume.

2.3. Fluorescent labeling

Different fluorescent labels used in this study are given in Table 2, below.

In our experimental procedures, a specific set of labels was utilized for each experiment, which will be detailed in the Materials and Methods section and the corresponding figure legends. In general, live neurons were differentiated and incubated with nanomaterial, followed by staining with fluorescent labels according to the manufacturers' guidelines.

It is noteworthy that CTG was the only label added one day prior to microscopy, while other

labels were added immediately before imaging. Additionally, only CTG was washed with PBS, whereas other labels were not washed. Antibodies used in this study will be described later in this section. Briefly, they were conjugated with fluorescent dyes and were added in specified concentrations just prior to microscopy.

Anti- A β antibodies are raised against amino acids 1–40 of β -Amyloid of human origin (<https://www.scbt.com/p/beta-amyloid-antibody-20-1>). The β -Amyloid Antibody (20.1) is a mouse monoclonal antibody of the IgG2b κ isotype specifically designed to target β -amyloid and amyloid precursor protein (APP) fragment from human sources.

The extracellular tau deposits were labeled with Tau (Tau-5) Mouse Monoclonal Antibody (Product # AHB0042) of IgG1 kappa κ isotype. It recognizes both phosphorylated and non- phosphorylated human tau proteins.

Both antibodies were added at $2\ \mu\text{g mL}^{-1}$ concentration to 7-day RA differentiated neurons in 1% BSA at 37°C. Imaging started immediately after the addition of antibodies.

2.4. Microscope setup

Following incubation with nanomaterial, the living samples were labeled and imaged using a state-of-the-art imaging system consisting of an Olympus (Olympus IX83) inverted microscope body equipped with a laser-scanning confocal and STED unit (Stedycon, Abberior). Stage top incubator (Okolab H301-MIN) maintains atmosphere with 37°C, 5% CO₂, and >95% humidity to enable long term imaging of living cells.

The images were captured using a confocal microscope equipped with either a 20x magnification objective and 0.8 numerical aperture (NA) lens or a 60x magnification objective with a 1.2 NA lens. The microscope system incorporates four pulsed

Table 2. List of fluorescent labels used in this study.

Fluorophore	Manufacturer (cat. nr)	Excitation peak (nm)	Emission peak (nm)	Concentration (μM)
CellTracker™ Green CMFDA (CTG)	Thermo Fisher (#C2925)	492	517	1
ATTO490 LS conjugated to anti-TAU ab	ATTO-TEC	495	658	0.01
CellMask™ Deep Red (CMDR)	Thermo Fisher (#C10046)	650	685	1
Alexa-647 conjugated to anti-A β ab	Thermo Fisher (#A20006)	650	665	0.01

laser sources (Abberior) with a pulse duration of 120 ps and a maximum power of 50 μ W at the sample plane. Additionally, four avalanche photodiode (APD) detectors are utilized for signal detection. The pulse repetition frequency was 80 MHz. The STED depletion laser, operating at a wavelength of 775 nm, had the same repetition frequency as the excitation lasers, a pulse duration of 1.2 ns, and a maximum power of 170 mW at the sample plane.

We detected nanoparticles in the label-free, backscatter detection mode, utilizing the 488/488 \pm 5 nm excitation/detection. Due to the large coherence of the laser, the backscattered light exhibited a strong speckle pattern, which was removed by Fourier transform bandpass filter (1–100 pixels) on scattering images. These images were subsequently binarized to obtain nanomaterial masks.

Please see the supplement for information regarding nanomaterial aggregation in cell medium, and automated-multi region of interest (ROI) data analysis and quantification of extracellular amyloid β containing plaques and neurite lengths.

3. Results and discussion

3.1. TiO₂ nanotubes trigger the formation of extracellular amyloid β , Tau, and neuronal cytosolic components containing plaques

Since anatase TiO₂ nanotubes induce retention of organic debris in alveolae with nanoparticles at the core of these deposits (Danielsen et al. 2020; Kokot et al. 2020), we tested whether the formation of similar deposits of organic molecules might occur inside the brain. We employed a human neuroblastoma cell line called SH-SY5Y, which is extensively utilized in studies due to their ability to differentiate into neuron-like cells. When differentiated, these cells exhibit characteristics resembling dopaminergic neurons found in the ventral hippocampus, which are involved in cognitive functions (Titulaer et al. 2021).

After the differentiation of SH-SY5Y, resulting in neuron-like cells with extensively branched neurites (Figure 1A, green) (Agholme et al. 2010; Kovalevich, Santerre, and Langford 2021; Kovalevich and Langford 2013), we exposed them to TiO₂ nanotubes (Figure 1A, red). Most of the added TiO₂ nanoparticles aggregate (Supplement Figure S1–S18) and settle to the glass surface never interacting with the cells (purely red signal in Figure 1A), whereas some portion of added nanoparticles, mostly single

nanotubes (Urbančić et al. 2018), translocate into the cells and gets excreted after a day (Kokot et al. 2020). We identified the nanoparticles that interact with cells by their co-localisation with the cytosolic label CellTracker™ Green CMFDA (CTG) (green, Figure 1B–D), with which we labeled the neurons prior to exposure. This label, once internalized by the cells, is acted upon by cellular esterases rendering it fluorescent throughout the cytoplasm. Without this interaction, it remains non fluorescent. In addition, thiol reactivity increases its intracellular retention through several generations (Beem and Segal 2013), thus precluding it from freely exiting the cells to adhere to the surface of TiO₂ nanotubes that had not interacted with the cells' interior.

Moreover, we observed that many of the above-mentioned aggregates also contained extracellular deposits of amyloid β (A β) peptide, as indicated by immunostaining with a mouse monoclonal antibody raised against amino acids 1–40 of A β of human origin, for detection of amyloid precursor protein and A β (Figure 1B–D, blue). Namely, aggregation of A β is a proteolytic product of amyloid precursor protein (A β PP) by β - and γ -secretases, resulting in two major A β isoforms: A β 42 (42 residues long) and A β 40 (40 residues long). Although the concentration of A β 40 in cerebral spinal fluid is several-fold higher than that of A β 42, the A β 42 is the predominant constituent of amyloid β plaques in AD brains (Iwatsubo et al. 1994, 1995), while A β 40 is present in only some of the plaques (Gravina et al. 1995; Mak et al. 1994), suggesting that initial plaque formation involves only A β 42 (Gu and Guo 2013). Therefore, we are aware of the limitation that quantifying only A β 40 might not be suitable for the detection of early A β containing plaques *in vitro*.

Phosphorylated Tau (p-tau) is also one of the biomarkers for the early stages of AD. For example, Tau phosphorylated at threonine-231 (T231) increase early in the preclinical stage of AD, probably in response to A β pathology (Suárez-Calvet et al. 2020). Therefore, we labeled the extracellular tau deposits with tau (Tau-5) mouse monoclonal antibody that should recognize both phosphorylated and non-phosphorylated human tau proteins (Figure 1B–D, white). Since cells can release Tau even if not exposed to a toxicant (Karch, Jeng, and Goate 2012), we cannot deduce whether nanoparticles bind Tau within a cell and transport it out or the cells release more Tau, which binds to nanoparticles outside of the cells. Tau is a neuronal microtubule-associated protein found predominantly in axons. The C-terminus binds axonal microtubules while the

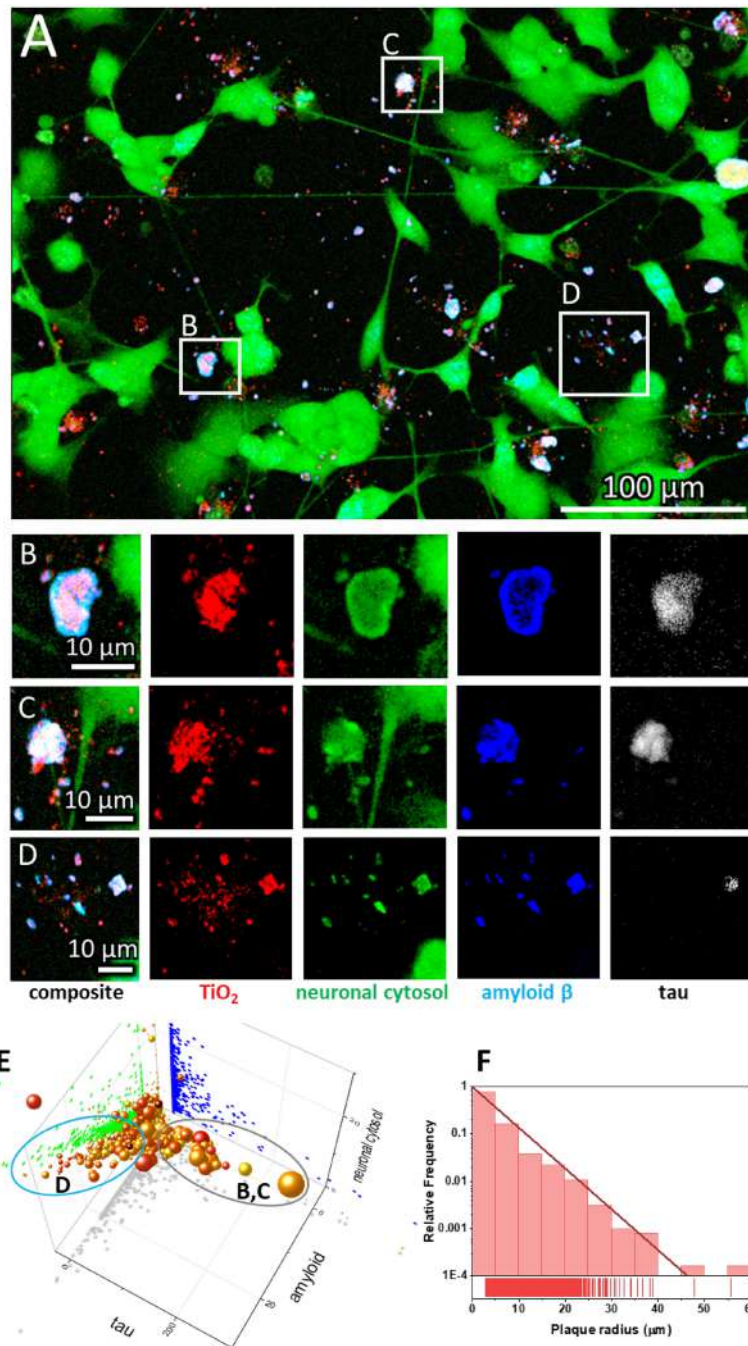


Figure 1. SH-SY5Y-derived neurons exposed to anatase TiO_2 nanotubes form amyloid- β and Tau protein-containing extracellular plaques. (A) Representative image of differentiated SH-SY5Y cells in culture; for differentiation, cells were grown for seven days in DMEM/F12, 10% fetal bovine serum, and $10\ \mu\text{M}$ retinoic acid, followed by 7 d in serum-free DMEM/F12 and $10\ \text{ng/mL}$ brain-derived neurotrophic factor. Note the altered morphology and pronounced neurite outgrowth upon differentiation. Live cell culture was stained with cytosolic fluorophore CellTracker™ green (green), which is retained and fluoresces only within a cell, a mouse monoclonal antibody raised against amino acids 1–40 of A β of human origin, for detection of amyloid precursor protein and A β (blue), and Tau-5 mouse monoclonal antibody against total Tau (white). Within the large field of view, the rectangles denote regions enlarged in the panels (B–D) showing examples of heterogeneous extracellular plaques at higher magnification: (B,C) large plaques with low A β surface density (fluorescence intensity signal divided by the area of the signal) and high tau surface density; (D) small plaques with high A β surface density and low tau surface density; (E) Properties of all the A β plaques from 15 regions of interest, each covering $120 \times 120\ \mu\text{m}^2$ in terms of surface densities with x-axis: tau antibody, y-axis: A β antibody, z-axis: neuronal cytosolic label, size of a sphere: plaque radius, and color: density of nanoparticles in a plaque, each sphere representing one plaque. Most of the nanomaterial is deposited on the glass surface without interacting with neurons (red), whereas the nanomaterial interacting with the neurons contains A β (blue), nanomaterial (red), and neuronal cytoplasmic components (green), while Tau (white) can be missing; the grey and blue ellipses denote plaques with high and low density of Tau, such as those in panels B/C and D, respectively. (F) The size distribution of the plaques, showing exponential decay of the number of plaques versus plaque size.

N-terminus binds neural plasma membrane components (Brandt, Léger, and Lee 1995; Padmanabhan et al. 2022). Many other roles for Tau were speculated (Sotiropoulos et al. 2017), including its role in insulin signaling (Marciniak et al. 2017) and being released extracellularly as a free protein (De La-Rocque et al. 2021), which can bind to receptors on living cells (Mudher et al. 2017), including amyloid precursor protein (Takahashi et al. 2015). Yet the precise mechanisms of tau pathology remain unanswered (Huiqin Zhang et al., 2021).

We observed the formation of extracellular deposits of A β and Tau (Figure 1 composite, white deposits near green neurons), which agrees with the current knowledge of extracellular plaque composition found in AD patients. There, two types of brain lesions are commonly observed: A β plaques and tau tangles, arising from the aggregation of misfolded A β and hyperphosphorylated tau proteins, respectively (Walker 2020). A β plaques have long been considered the initial event of the disease process (Leng and Edison 2021). However, recent studies have shown that A β plaques can act as seeds for the initial Tau accumulation into large aggregates containing both proteins. This initial accumulation occurs in dystrophic neurites surrounding A β plaques, referred to as neuritic plaque tau (NP Tau), consistent with imaging studies and investigations of postmortem AD brains (He et al. 2018). Our data (Figure 1B–D) corroborates this notion, showing protein deposits containing both A β and tau protein, resembling structures observed in mice and patients by He et al. (2018).

To examine the heterogeneity of extracellular A β plaques, we analyzed 15 regions of interest (ROI), each covering $120 \times 120 \mu\text{m}^2$. An example of the algorithm we used for calculating densities of plaque components is shown in the supplement (Figure S21). We identified more than six thousand plaques, the properties of which are plotted in a 5-dimensional graph in Figure 1E. As the x coordinate, we assigned the A β signal density (fluorescence signal intensity divided by the surface area of an extracellular deposit=plaque), as y coordinate, we assigned the Tau signal density, and as z coordinate, we assigned the cytoplasmic signal density. In this way one can see that some of the points lie in the xz plane ($y=0$, no tau signal), yet there are no points in the xy ($z=0$) and yz ($x=0$) plane indicating that all extracellular deposits contain A β (blue) and cytoplasm of neurons (green). Each sphere in the graph represents one plaque,

with the size of the sphere proportional to the plaque radius and the color representing the density of the nanomaterial according to the color scale. Interestingly, some plaques lack Tau (x axis), whereas others contain lots of it. This observation aligns with the heterogeneous nature of plaques found in AD patients, where there is high diversity in all plaque components except for A β , which is universally present in all plaques (Walker 2020).

Notably, the amount of A β in our plaques is proportional to the amount of cytosolic label observed, indicating that the neurons generate A β because fluorescing cell tracker label must have originated from neuronal cytoplasm (Figure 1E distribution of green dots in an amyloid-neuronal cytosol plane). This is in accordance with the finding that plaque formation initiates within the neuron, and subsequential accumulation of fibrillar A β occurs intraluminally (Le Bras 2022; Lee et al. 2022; Pensalfini et al. 2014). Furthermore, many other cell proteins have been identified within A β plaques. For example, a comparison of biomolecules in A β plaques (amyloidome) of human A β plaque regions versus non-plaque regions of AD and healthy controls revealed significantly higher levels of neuronal proteins (Bai et al. 2021; Drummond et al. 2017; Xiong, Ge, and Ma 2019), further strengthening the idea that the plaque initially forms within the neuron.

The number of the plaques decreases exponentially with the radius of a plaque (Figure 1F), with the characteristic length of $3.3 \mu\text{m}$ and most plaques having a radius below $40 \mu\text{m}$, corresponding to a cross-section area of $5000 \mu\text{m}^2$. Such a size distribution, including exponential behavior and maximum size, is similar to the distribution of A β oligomeric structures observed *in vitro* on lipid membranes by Tahirbegi et al. (Tahirbegi et al. 2020). However, the plaque sizes we observed are larger than suggested by Serrano-Pozo et al., who showed that in AD, patients maximum plaque sizes reach up to $500 \mu\text{m}^2$ (Serrano-Pozo et al. 2012). We speculate this difference might be due to the absence of microglia in our cell culture model, as the microglia are known to influence plaque formation (Bai et al. 2021; Leng and Edison 2021). For example, Shabestari et al. showed that re-engraftment the population of microglia in AD mice brains resulted in the formation of more compact, smaller plaques (Kiani Shabestari et al. 2022). Nevertheless, the size of plaques seems to be loosely governed by the density of Tau and A β proteins within them. Larger plaques tend to have a higher density of

Tau, and smaller ones have higher A β density (Figure 1D).

3.2. Amyloid β (A β) plaques form at the sites of damaged neurites

Above we have shown that exposure to nanoparticles can trigger the formation of A β plaques, possibly due to the direct damage to neurons, as evidenced by the presence of Tau and neuronal cytosolic components within the plaques. This is not that surprising considering our previous studies where we showed that these nanotubes can disturb plasma membrane (Urbančič et al. 2018) and cytosolic organelles (Kokot et al. 2020), including microtubule structure, within minutes after exposure. We next conducted high temporal and spatial resolution imaging of neurite morphology at different confocal planes (Figure 2A,B) to investigate whether nanotubes can directly damage the neurites they contact. Next to an exemplary A β plaque that spans a height of 3 μ m, we observed an axon extending from the neuron body at the lowest z plane (Figure 2B, z=0 μ m) that stopped at the A β plaque. Interestingly, another axon above the first remained intact and reached over the plaque three μ m above the lowest point (Figure 2B, z=3 μ m).

To gain a better understanding of these observations, we employed long-term time-lapse monitoring of neurites (Figure 2C, green) to discover that TiO₂ nanotube aggregates (red) quickly colocalized with components of neuronal cytosol get (yellow, overlap of red and green), leading to discontinuation of a neurite within minutes after exposure as indicated by the yellow arrows in Figure 2C. Furthermore, high-resolution imaging using stimulated emission depletion (STED) microscopy revealed damaged synapses (green) where nanotubes (red) concentration was the highest (Figure 2D, white arrows). We also observed an early formation of a plaque near the neurite containing nanoparticles (red, Figure 2D, STED zoom-in NANO), neuronal plasma membrane components (green, MEMBRANE), and A β (blue, A β). Conversely, in the absence of TiO₂ nanotubes, neurites of that same axon retained their integrity and no A β was detected in their proximity.

3.3. Diesel exhaust and iron oxide nanoparticles induce the most neurite shortening

Despite a strong epidemiological correlation between exposure to airborne particulate matter

and the development of neurodegenerative diseases (Peeples 2020; Shi et al. 2020, 2021), the causal relationship between particulate matter in air pollution and A β plaque deposition with neurite degeneration in AD remains controversial (Budson 2020; Underwood 2017). To address this, we investigated whether various types of particulate matter commonly found in polluted air, including metal oxides and carbonaceous particles, could trigger the formation of A β plaques and neurite shortening as observed above for the TiO₂ nanotubes.

For this purpose, we compared the effect of TiO₂ nanotubes, CeO₂, γ -Fe₂O₃, and diesel exhaust particles on neurite lengths and their number in neuronal cell culture (Figure 3). We analyzed neurite lengths at 1 and 100 h after exposure to these materials using the Fiji ImageJ with NeuronJ plug-in, a program that can be used for semi-automated tracing of individual neurons (Popko et al. 2009). Representative images of chosen neurites, each connecting two distinct cells, are shown in violet in Figure 3 and in the supplement Section 5. The extracted distribution of neurite lengths across multiple images are plotted in the right-most column in Figure 3.

After 100 hours of exposure to nanomaterials, a significant reduction occurred in median length of neurites in neurons exposed to TiO₂ nanotubes (from 59.4 μ m to 39.8 μ m, $p < 0.001$), γ -Fe₂O₃ (from 56.8 μ m to 32.2 μ m, $p < 0.001$), and diesel exhaust particles (from 60.7 μ m to 29.6 μ m, $p < 0.001$), compared to the same sample after 1-hour exposure. In contrast, CeO₂ did not exhibit any reduction in length even after 100 h, compared the measurements taken an hour after exposure (Mann–Whitney U test applied due to the non-normal distribution of data). We observed the greatest effect in γ -Fe₂O₃ and diesel exhaust particles exposed neurons, where the median length decreased almost to a half of that observed in control. Alongside, the relative proportion of short neurites (<10 μ m) dramatically increased, while there were almost no very long neurites (>100 μ m) left (see histograms of number of neurites (n) versus neurite length in Figure 3 right).

3.4. Amyloid β (A β) plaques might have a protective role in neuronal survival after nanomaterial exposure

To gain insight into why some types of particulate matter (CeO₂) do not affect neurite lengths and density to such an extent as other types (TiO₂ nanotubes, γ -Fe₂O₃ and diesel exhaust particles) we

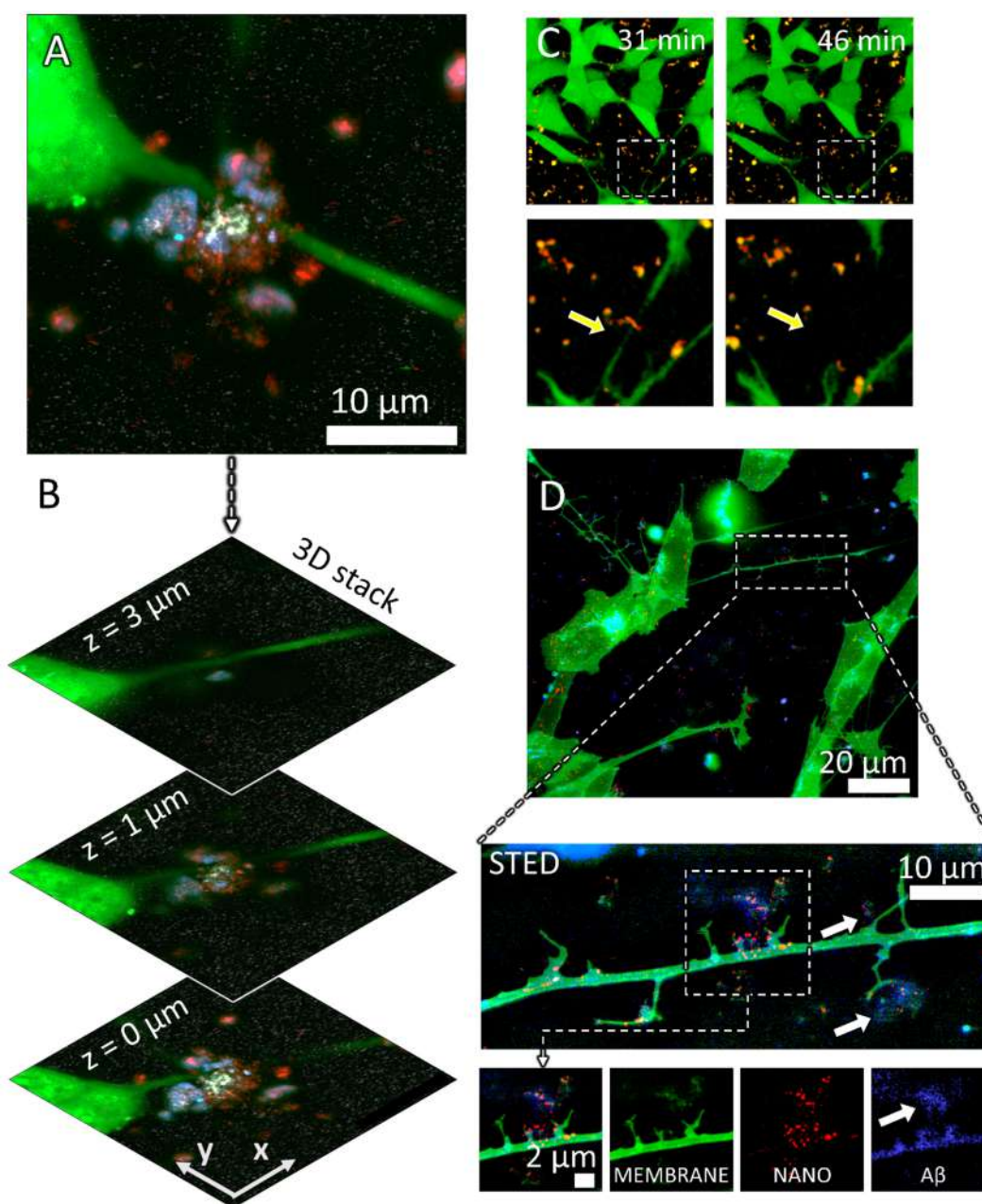


Figure 2. Neurite dystrophy and early amyloid β plaque formation at the sites of retracted neurites caused by anatase TiO_2 nanotubes. (A) a maximum intensity projection image of the confocal planes in (B) Composite confocal fluorescence image of an $\text{A}\beta$ containing plaque at three different z heights from the signal of probes for neuronal cytosol (green), TiO_2 nanotubes (red), $\text{A}\beta$ (blue), and Tau (white); (C) live cell imaging of neurite collapse occurring within minutes after nanoparticle exposure, arrow points to a neurite that collapses in contact with the nanotubes; (D) neuronal plasma membrane labeled with CellMask™ deep red (CMDR) (green), high spatial resolution fluorescence image (stimulated emission depletion STED) of synapse damage and early plaque formation (white arrows) at the sites of damaged synapses (green, MEMBRANE) by the nanotubes (red, NANO) containing $\text{A}\beta$ (blue, $\text{A}\beta$).

analyzed the amount of $\text{A}\beta$ deposited after nanomaterial exposure and assessed its colocalization with nanomaterial (Figure 4).

We first notice that all types of particles, except CeO_2 nanoparticles (Figure 4B), trigger the release of $\text{A}\beta$ (compare the height of blue bars in Figure 4G and the intensities of blue signal in Figure 4A–E).

TiO_2 nanotubes triggered the formation of the large plaques containing neuronal plasma membrane (green), nanomaterial (red), and $\text{A}\beta$ (blue), resulting in the overlapping signal of all three colors (Figure 4C, light pink). TiO_2 nanotubes were also the most efficiently covered with $\text{A}\beta$, up to about 80% (pink spheres in Figure 4F).

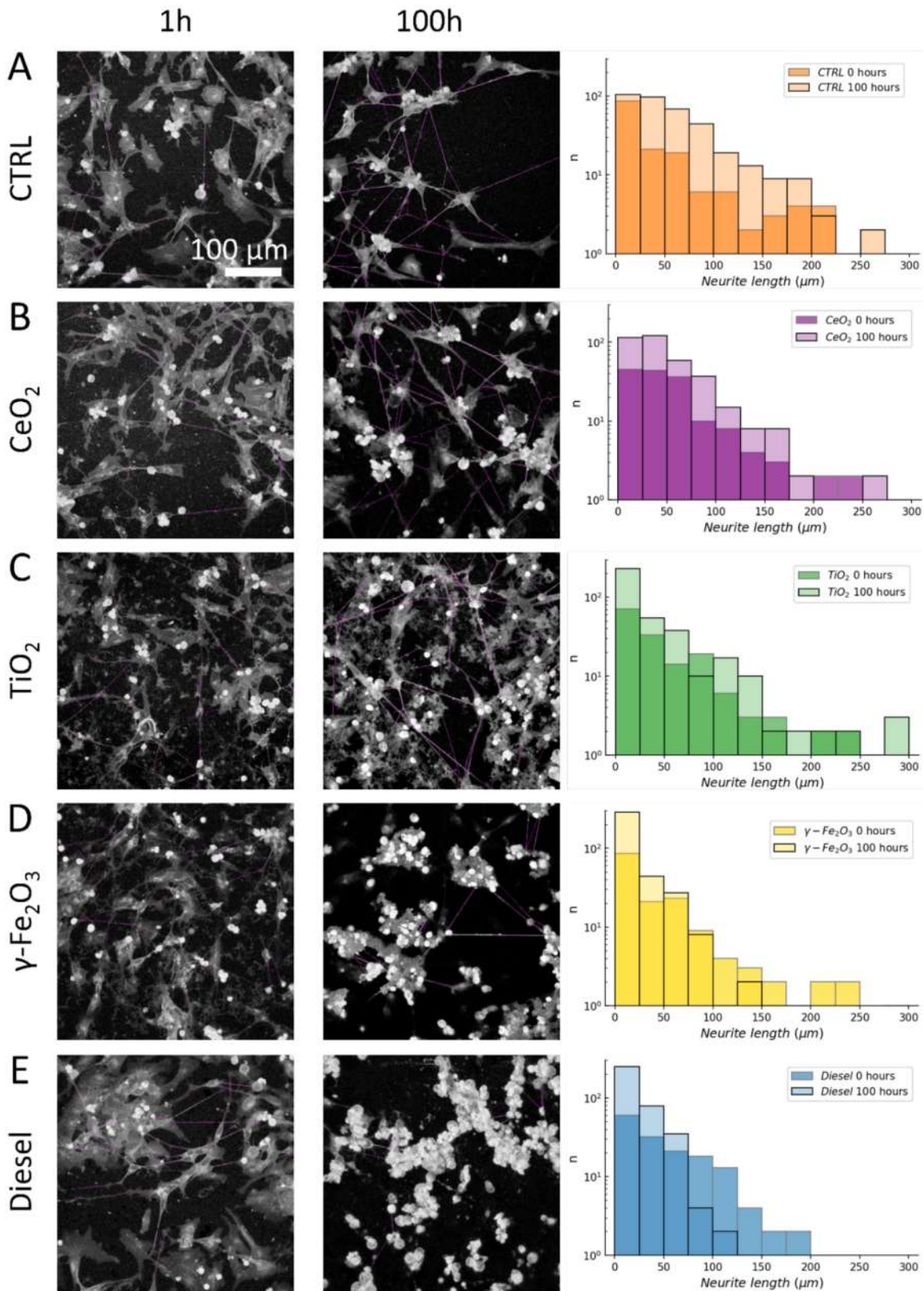


Figure 3. Neurite length shortening from 1 h to 100 h after exposure to nanomaterial. We determined the lengths of neurites that connected two distinct neuronal cells at 1 and 100 h after exposure to nanomaterials using the NeuronJ plug-in. Representative images of neurites selected for analysis are shown in violet in the left (1 h) and Middle (100 h) column. The right-most column shows the distributions of neurite lengths 1 h (transparent) and 100 h (solid with black edges) after exposure to different nanomaterials: (A) control, (B) TiO₂ nanotubes, (C) CeO₂, (D) γ -Fe₂O₃, and (E) diesel exhaust particles exposed neurons. Median values of neurite lengths of all samples were significantly shortened for TiO₂ nanotubes, γ -Fe₂O₃, and diesel exhaust particles ($p < 0.001$, Mann-Whitney U test).

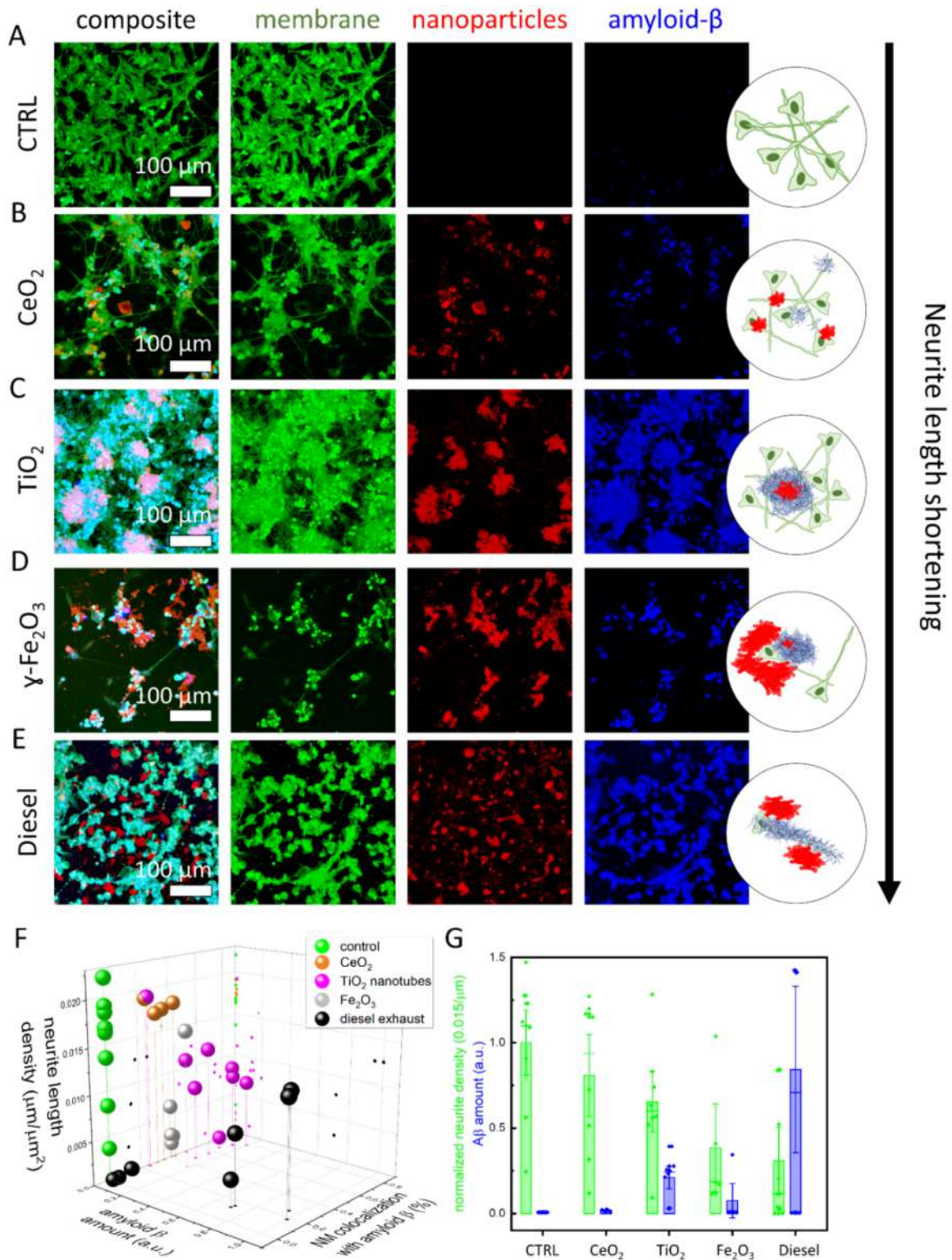


Figure 4. Particulate matter triggered amyloid β -containing plaques in neuronal cell culture 2 days after exposure to a nanomaterial. Confocal images of differentiated SH-SY5Y live neuronal cells were stained with fluorescent CellMask™ deep red dye (membrane, green), unlabeled nanoparticles were detected via scattering (nanoparticles, red), A β plaques were immunostained with mouse monoclonal anti- β -amyloid antibody (santa cruzblue, # sc-53822; blue color) conjugated with ATTO490 LS, antibodies were added to living cells in 10 nM concentration. (A) control – unexposed neurons; (B) neurons exposed to TiO₂ nanotubes; (C) CeO₂ nanoparticles; (D) γ -Fe₂O₃ nanoparticles; (E) Diesel exhaust particles; (F) neurite length density (z axis), amount of A β (x axis), and proportion of nanoparticles colocalized with A β (y axis), each symbol represents values obtained from one ROI; (G) neurite density was calculated as total neurite length per total area (green bars), amount of A β was estimated as an integral of fluorescence intensity signal of A β antibody (blue bars), each symbol represents value obtained from one region of interest (ROI with a size of 400 μ m \times 400 μ m, the height of the bar represents mean value, whiskers are standard deviation, long horizontal line is the median).

On the other hand, iron oxide and diesel exhaust particles colocalized less with A β , about 40% and less than 20% on average, respectively (gray and black spheres in Figure 4F). In addition, diesel exhaust also triggered the highest release of A β (blue bar in Figure 4G), but these aggregates colocalized with neurons rather than the nanoparticles themselves (Figure 4E; cyan color indicated colocalization of plasma membrane and A β signal). Furthermore, diesel exhaust particles caused massive neuronal death across the whole sample, as indicated by the presence of numerous rounded neurons with high membrane label intensity and no axons in Figure 4E. Such effects were also observed by others in a coculture system (Block et al. 2004; Seo et al. 2023). Interestingly, in the regions where the amount of A β deposits was high and diesel exhaust particles colocalized with A β deposits, the lengths of neurites were about ten times longer compared to regions with minimal A β deposition. Each such region is presented by a black sphere with higher A β amount values in Figure 4F. One can therefore see two groups of black spheres indicating the potential protective role of A β accumulation at the diesel exhaust particles. We speculate that this observation could potentially provide a mechanistic explanation to the conundrum observed in AD patients who possess a high burden of A β plaques but do not experience adverse symptoms (Gómez-Isla and Frosch 2022).

In Figure 4G, we show that exposure to nanomaterials that induce higher A β deposits (blue bars) generally leads to shortening of neurites (green bars) compared to the control. Despite inducing more A β deposits than γ -Fe $_2$ O $_3$ nanoparticles, TiO $_2$ nanotubes cause less neurite loss. This discrepancy might be attributed to the property of TiO $_2$ nanotubes to bind more A β , thus again highlighting a protective role of A β deposition surrounding the nanomaterial.

These findings suggest that A β plaque formation does not necessarily coincide with neurite loss, which could explain why not all individuals with plaques develop AD (Gómez-Isla and Frosch 2022), as well as why numerous clinical trials directed at reducing A β have failed in humans, despite their success in genetic mouse models of AD. Namely, it has been proposed that the reason for the failures of clinical trials in humans is that mouse models only exhibit plaques without other hallmarks of the disease, whereas AD patients develop plaques, tau deposits, and neuronal degeneration (Busche and Hyman 2020). Therefore, the induction of A β and

tau plaque formation accompanied by neurite atrophy and neuronal degeneration through particulate matter exposure might represent a more relevant model of AD compared to existing genetically induced mouse models.

3.5. Conclusion

We here report the formation of extracellular A β plaques, resembling those found in AD, after exposure of an *in vitro* neuronal cell culture to engineered anatase TiO $_2$ nanotubes, which we previously showed to trigger chronic lung inflammation and nanoparticle-containing organic debris formation in mice (Danielsen et al. 2020; Kokot et al. 2020). These plaques closely resemble those in mice and AD patients observed by He et al. (He et al. 2018), which were induced in wild-type mice via intracerebral injection of Tau. Here we show that similar plaques can be triggered with exposure to some nanomaterials. We exposed SH-SY5Y-derived human neurons to a very high dose of engineered anatase TiO $_2$ nanotubes and monitored the formation of A β and Tau-containing plaques 24–48 h later. TiO $_2$ nanotubes caused neurites (i.e. cellular protrusions extending from neurons) to shorten (median length decreased from 59.4 μ m to 39.8 μ m, $p < 0.001$) and atrophy (Figure 2C,D), causing a decrease in neurite lengths (Figure 3C). Oppositely, CeO $_2$ nanoparticles do not cause neurite shortening (Figure 3B) and do not induce A β plaque formation, which is consistent with their beneficial effect observed in traumatic brain injury (Fiorani et al. 2015; Gagnon and Fromm 2015).

We also tested other nanomaterials that can be found in polluted air, diesel exhaust and iron oxide particles, which are associated with cognitive decline in areas with high air pollution (Underwood 2017). Iron oxide (γ -Fe $_2$ O $_3$ (from 56.8 μ m to 32.2 μ m, $p < 0.001$)) and diesel exhaust particles (from 60.7 μ m to 29.6 μ m, $p < 0.001$), decreased neurite lengths the most (Figure 3C) and induced the accumulation of A β mainly in apoptotic neurons, as suggested by their rounded-up morphology, typical of apoptotic cells. On the other hand, TiO $_2$ nanotubes induced the accumulation of A β in extracellular space often co-localized with the nanoparticles, suggesting that aggregation of the nanoparticles with A β might be a protective mechanism that ‘hides’ the material’s surface and prevents its harmful contact with neurons, thus safeguarding neurites.

Overall, this study identifies how certain nanoparticles relevant to particulate matter in ambient air

pollution might contribute to AD by triggering hallmarks of the disease: shortening of neurites, formation of A β plaques and, in the case of TiO₂, accumulation of Tau protein within these plaques. Furthermore, we speculate that A β plaque colocalization with a nanomaterial could potentially protect neurites. While the exact mechanism behind this effect remains to be explained, it is possible that exposure to different types of ambient air pollution could explain earlier observations of individuals experiencing a high burden of plaques yet no adverse cognitive symptoms (Gómez-Isla and Frosch 2022).

Acknowledgments

Louise Gren, Polona Umek, and Martí Busquets Fité are acknowledged for providing TEM images of diesel exhaust, TiO₂, and CeO₂ particles, respectively.

Authors contributions

Conceptualization and design: A.S., T.K., I.U. and J.Š.; data collection: A.S.; analysis and interpretation of the data: A.S., T.K., I.U. and J.Š.; the drafting of the paper: A.S., T.K.; revising the paper critically for intellectual content: A.S., L.M.A.C., V. M., S.K., J.P., U.V., S.Z.N., I.U., T.K., and J.Š.; All authors gave the final approval of the version to be published; all authors agree to be accountable for all aspects of the work.

Disclosure statement










No potential conflict of interest was reported by the author(s).

Funding

The authors acknowledge the financial support from the Slovenian Research Agency (research core funding No. P1-0060 Experimental biophysics of complex systems and imaging in biomedicine, and No. P2-0089). The authors acknowledge the projects (Intelligent Content-Aware Nanospectroscopy (iCAN) of molecular events in nanoparticles-induced neurodegeneration, J7-2596, Concept development for mechanistic prediction of fibrosis and initiation of blood coagulation induced by inhaled materials (uCellnNet), N1-0240, L7-4535, J2-3043, J2-3040, J2-3046, J3-3079, and J7-4420, and bilateral ARRS project No. BI-FR/23-24-PROTEUS-005 (PR-12039), BI-US/22-24-100) financially supported by the Slovenian Research and Innovation Agency (SRA-ARIS). This work was also funded by European Union (grant no. 101092741, nanoPASS).

ORCID

Aleksandar Sebastijanović  <http://orcid.org/0000-0003-0400-7974>

Laura Maria Azzurra Camassa  <http://orcid.org/0000-0002-5041-942X>
 Vilhelm Malmberg  <http://orcid.org/0000-0002-4362-1646>
 Slavko Kralj  <http://orcid.org/0000-0002-0771-3818>
 Joakim Pagels  <http://orcid.org/0000-0002-7423-3240>
 Ulla Vogel  <http://orcid.org/0000-0001-6807-1524>
 Shan Zienolddiny-Narui  <http://orcid.org/0000-0001-9747-9625>
 Iztok Urbančič  <http://orcid.org/0000-0003-3603-6585>
 Tilen Koklič  <http://orcid.org/0000-0002-6085-7060>
 Janez Štrancar  <http://orcid.org/0000-0001-8032-132X>

Data availability statement

The authors confirm that the data supporting the findings of this study are available upon request within the article and its [supplementary materials](#).

References

- Agholme, L., T. Lindström, K. Kågedal, J. Marcusson, and M. Hallbeck. 2010. "An in Vitro Model for Neuroscience: Differentiation of SH-SY5Y Cells into Cells with Morphological and Biochemical Characteristics of Mature Neurons." *Journal of Alzheimer's Disease* 20 (4): 1069–1082. <https://doi.org/10.3233/JAD-2010-091363>.
- Bai, B., D. Vanderwall, Y. Li, X. Wang, S. Poudel, H. Wang, K. K. Dey, P.-C. Chen, K. Yang, and J. Peng. 2021. "Proteomic Landscape of Alzheimer's Disease: Novel Insights into Pathogenesis and Biomarker Discovery." *Molecular Neurodegeneration* 16 (1): 55. <https://doi.org/10.1186/s13024-021-00474-z>.
- Baj, J., B. Kowalska, W. Flieger, E. Radzikowska-Büchner, A. Forma, M. Czezelewski, P. Kędzierawski, et al. 2023. "Assessment of the Concentration of 51 Elements in the Liver and in Various Parts of the Human Brain—Profiling of the Mineral Status." *Nutrients* 15 (12): 2799. <https://doi.org/10.3390/nu15122799>.
- Beem, E., and M. S. Segal. 2013. "Evaluation of Stability and Sensitivity of Cell Fluorescent Labels When Used for Cell Migration." *Journal of Fluorescence* 23 (5): 975–987. <https://doi.org/10.1007/s10895-013-1224-8>.
- Bendtsen, K. M., L. Gren, V. B. Malmberg, P. C. Shukla, M. Tunér, Y. J. Essig, A. M. Kraiss, et al. 2020. "Particle Characterization and Toxicity in C57BL/6 Mice following Instillation of Five Different Diesel Exhaust Particles Designed to Differ in Physicochemical Properties." *Particle and Fibre Toxicology* 17 (1): 38. <https://doi.org/10.1186/s12989-020-00369-9>.
- Blennow, K., M. J. de Leon, and H. Zetterberg. 2006. "Alzheimer's Disease." *Lancet* 368 (9533): 387–403. [https://doi.org/10.1016/S0140-6736\(06\)69113-7](https://doi.org/10.1016/S0140-6736(06)69113-7).
- Block, M. L., X. Wu, Z. Pei, G. Li, T. Wang, L. Qin, B. Wilson, J. Yang, J. S. Hong, and B. Veronesi. 2004. "Nanometer Size Diesel Exhaust Particles Are Selectively Toxic to Dopaminergic Neurons: The Role of Microglia, Phagocytosis, and NADPH Oxidase." *FASEB Journal* 18 (13): 1618–1620. <https://doi.org/10.1096/fj.04-1945fj>.
- Brandt, R., J. Léger, and G. Lee. 1995. "Interaction of Tau with the Neural Plasma Membrane Mediated by Tau's

- Amino-Terminal Projection Domain." *The Journal of Cell Biology* 131 (5): 1327–1340. <https://doi.org/10.1083/jcb.131.5.1327>.
- Budson, A. E. 2020. "Does air Pollution Cause Alzheimer's Disease?" *Harvard Health Blog*. <https://www.health.harvard.edu/blog/does-air-pollution-cause-alzheimers-disease-2020072320627>
- Busche, M. A., and B. T. Hyman. 2020. "Synergy between Amyloid- β and Tau in Alzheimer's Disease." *Nature Neuroscience* 23 (10): 1183–1193. <https://doi.org/10.1038/s41593-020-0687-6>.
- Calderón-Garcidueñas, L., and A. Ayala. 2022. "Air Pollution, Ultrafine Particles, and Your Brain: Are Combustion Nanoparticle Emissions and Engineered Nanoparticles Causing Preventable Fatal Neurodegenerative Diseases and Common Neuropsychiatric Outcomes?" *Environmental Science & Technology* 56 (11): 6847–6856. <https://doi.org/10.1021/acs.est.1c04706>.
- Calderón-Garcidueñas, L., A. Herrera-Soto, N. Jury, B. A. Maher, A. González-Maciél, R. Reynoso-Robles, P. Ruiz-Rudolph, B. van Zundert, and L. Varela-Nallar. 2020. "Reduced Repressive Epigenetic Marks, Increased DNA Damage and Alzheimer's Disease Hallmarks in the Brain of Humans and Mice Exposed to Particulate Urban Air Pollution." *Environmental Research* 183: 109226. <https://doi.org/10.1016/j.envres.2020.109226>.
- Carey, I. M., H. R. Anderson, R. W. Atkinson, S. D. Beevers, D. G. Cook, D. P. Strachan, D. Dajnak, J. Gulliver, and F. J. Kelly. 2018. "Are Noise and Air Pollution Related to the Incidence of Dementia? A Cohort Study in London, England." *BMJ Open* 8 (9): e022404. <https://doi.org/10.1136/bmjopen-2018-022404>.
- Couzin-Frankel, J. 2023. "Promising Alzheimer's Therapies Shrink Brains." *Science (New York, N.Y.)* 380 (6640): 19–19. <https://doi.org/10.1126/science.adi1220>.
- Danielsen, P. H., K. B. Knudsen, J. Štrancar, P. Umek, T. Koklič, M. Garvas, E. Vanhala, et al. 2020. "Effects of Physicochemical Properties of TiO₂ Nanomaterials for Pulmonary Inflammation, Acute Phase Response and Alveolar Proteinosis in Intratracheally Exposed Mice." *Toxicology and Applied Pharmacology* 386: 114830. <https://doi.org/10.1016/j.taap.2019.114830>.
- De La-Rocque, S., E. Moretto, I. Butnaru, and G. Schiavo. 2021. "Knockin' on Heaven's Door: Molecular Mechanisms of Neuronal Tau Uptake." *Journal of Neurochemistry* 156 (5): 563–588. <https://doi.org/10.1111/jnc.15144>.
- Debia, M., C. Couture, P.-E. Njanga, E. Neesham-Grenon, G. Lachapelle, H. Coulombe, S. Hallé, and S. Aubin. 2017. "Diesel Engine Exhaust Exposures in Two Underground Mines." *International Journal of Mining Science and Technology* 27 (4): 641–645. <https://doi.org/10.1016/j.ijmst.2017.05.011>.
- Drew, L. 2018. "An Age-Old Story of Dementia." *Nature* 559 (7715): S2–S3. <https://doi.org/10.1038/d41586-018-05718-5>.
- Drummond, E., S. Nayak, A. Faustin, G. Pires, R. A. Hickman, M. Askenazi, M. Cohen, et al. 2017. "Proteomic Differences in Amyloid Plaques in Rapidly Progressive and Sporadic Alzheimer's Disease." *Acta Neuropathologica* 133 (6): 933–954. <https://doi.org/10.1007/s00401-017-1691-0>.
- Du, Z., M. Li, J. Ren, and X. Qu. 2021. "Current Strategies for Modulating A β Aggregation with Multifunctional Agents." *Accounts of Chemical Research* 54 (9): 2172–2184. <https://doi.org/10.1021/acs.accounts.1c00055>.
- Eftekharzadeh, B., B. T. Hyman, and S. Wegmann. 2016. "Structural Studies on the Mechanism of Protein Aggregation in Age Related Neurodegenerative Diseases." *Mechanisms of Ageing and Development* 156: 1–13. <https://doi.org/10.1016/j.mad.2016.03.001>.
- Falke, E., J. Nissanov, T. W. Mitchell, D. A. Bennett, J. Q. Trojanowski, and S. E. Arnold. 2003. "Subicular Dendritic Arborization in Alzheimer's Disease Correlates with Neurofibrillary Tangle Density." *The American Journal of Pathology* 163 (4): 1615–1621. [https://doi.org/10.1016/S0002-9440\(10\)63518-3](https://doi.org/10.1016/S0002-9440(10)63518-3).
- Finnegan, M. E., N. P. Visanji, I. Romero-Canelon, E. House, S. Rajan, J. F. W. Mosselmans, L.-N. Hazrati, J. Dobson, and J. F. Collingwood. 2019. "Synchrotron XRF Imaging of Alzheimer's Disease Basal Ganglia Reveals Linear Dependence of High-Field Magnetic Resonance Microscopy on Tissue Iron Concentration." *Journal of Neuroscience Methods* 319: 28–39. <https://doi.org/10.1016/j.jneumeth.2019.03.002>.
- Fiorani, L., M. Passacantando, S. Santucci, S. Di Marco, S. Bisti, and R. Maccarone. 2015. "Cerium Oxide Nanoparticles Reduce Microglial Activation and Neurodegenerative Events in Light Damaged Retina." *PLOS One* 10 (10): e0140387. <https://doi.org/10.1371/journal.pone.0140387>.
- Gagnon, J., and K. M. Fromm. 2015. "Toxicity and Protective Effects of Cerium Oxide Nanoparticles (Nanoceria) Depending on Their Preparation Method, Particle Size, Cell Type, and Exposure Route." *European Journal of Inorganic Chemistry* 2015 (27): 4510–4517. <https://doi.org/10.1002/ejic.201500643>.
- Glennier, G. G., and C. W. Wong. 1984. "Alzheimer's Disease: initial Report of the Purification and Characterization of a Novel Cerebrovascular Amyloid Protein." *Biochemical and Biophysical Research Communications* 120 (3): 885–890. [https://doi.org/10.1016/s0006-291x\(84\)80190-4](https://doi.org/10.1016/s0006-291x(84)80190-4).
- Gómez-Isla, T., and M. P. Frosch. 2022. "Lesions without Symptoms: Understanding Resilience to Alzheimer Disease Neuropathological Changes." *Nature Reviews Neurology* 18 (6): 323–332. <https://doi.org/10.1038/s41582-022-00642-9>.
- Gravina, S. A., L. Ho, C. B. Eckman, K. E. Long, L. Otvos, L. H. Younkin, N. Suzuki, and S. G. Younkin. 1995. "Amyloid Beta Protein (a Beta) in Alzheimer's Disease Brain. Biochemical and Immunocytochemical Analysis with Antibodies Specific for Forms Ending at a Beta 40 or a Beta 42(43)." *The Journal of Biological Chemistry* 270 (13): 7013–7016. <https://doi.org/10.1074/jbc.270.13.7013>.
- Gren, L., V. B. Malmborg, N. R. Jacobsen, P. C. Shukla, K. M. Bendtsen, A. C. Eriksson, Y. J. Essig, et al. 2020. "Effect of Renewable Fuels and Intake O₂ Concentration on Diesel Engine Emission Characteristics and Reactive Oxygen Species (ROS) Formation." *Atmosphere* 11 (6): 641. <https://doi.org/10.3390/atmos11060641>.
- Gu, L., and Z. Guo. 2013. "Alzheimer's A β 42 and A β 40 Peptides Form Interlaced Amyloid Fibrils." *Journal of Neurochemistry* 126 (3): 305–311. <https://doi.org/10.1111/jnc.12202>.
- He, Z., J. L. Guo, J. D. McBride, S. Narasimhan, H. Kim, L. Changolkar, B. Zhang, et al. 2018. "Amyloid- β Plaques Enhance Alzheimer's Brain Tau-Seeded Pathologies by Facilitating Neuritic Plaque Tau Aggregation." *Nature Medicine* 24 (1): 29–38. <https://doi.org/10.1038/nm.4443>.

- Iwatsubo, T., D. M. Mann, A. Odaka, N. Suzuki, and Y. Ihara. 1995. "Amyloid Beta Protein (a Beta) Deposition: A Beta 42(43) Precedes a Beta 40 in Down Syndrome." *Annals of Neurology* 37 (3): 294–299. <https://doi.org/10.1002/ana.410370305>.
- Iwatsubo, T., A. Odaka, N. Suzuki, H. Mizusawa, N. Nukina, and Y. Ihara. 1994. "Visualization of a Beta 42(43) and a Beta 40 in Senile Plaques with End-Specific a Beta Monoclonals: Evidence That an Initially Deposited Species is a Beta 42(43)." *Neuron* 13 (1): 45–53. [https://doi.org/10.1016/0896-6273\(94\)90458-8](https://doi.org/10.1016/0896-6273(94)90458-8).
- Karch, C. M., A. T. Jeng, and A. M. Goate. 2012. "Extracellular Tau Levels Are Influenced by Variability in Tau That is Associated with Tauopathies." *The Journal of Biological Chemistry* 287 (51): 42751–42762. <https://doi.org/10.1074/jbc.M112.380642>.
- Karran, E., M. Mercken, and B. D. Strooper. 2011. "The Amyloid Cascade Hypothesis for Alzheimer's Disease: An Appraisal for the Development of Therapeutics." *Nature Reviews Drug Discovery* 10 (9): 698–712. <https://doi.org/10.1038/nrd3505>.
- Kiani Shabestari, S., S. Morabito, E. P. Danhash, A. McQuade, J. R. Sanchez, E. Miyoshi, J. P. Chadarevian, et al. 2022. "Absence of Microglia Promotes Diverse Pathologies and Early Lethality in Alzheimer's Disease Mice." *Cell Reports* 39 (11): 110961. <https://doi.org/10.1016/j.celrep.2022.110961>.
- Kokot, H., B. Kokot, A. Sebastijanović, C. Voss, R. Podlipec, P. Zawilska, T. Berthing, et al. 2020. "Prediction of Chronic Inflammation for Inhaled Particles: The Impact of Material Cycling and Quarantining in the Lung Epithelium." *Advanced Materials* 32 (47): 2003913. <https://doi.org/10.1002/adma.202003913>.
- Kovalevich, J., and D. Langford. 2013. "Considerations for the Use of SH-SY5Y Neuroblastoma Cells in Neurobiology." *Methods in Molecular Biology* 1078: 9–21. https://doi.org/10.1007/978-1-62703-640-5_2.
- Kovalevich, J., M. Santerre, and D. Langford. 2021. "Considerations for the Use of SH-SY5Y Neuroblastoma Cells in Neurobiology." *Methods in Molecular Biology* 2311: 9–23. https://doi.org/10.1007/978-1-0716-1437-2_2.
- Kralj, S., and D. Makovec. 2014. "The Chemically Directed Assembly of Nanoparticle Clusters from Superparamagnetic Iron-Oxide Nanoparticles." *RSC Advances* 4 (25): 13167–13171. <https://doi.org/10.1039/c4ra00776j>.
- Kralj, S., M. Rojnik, R. Romih, M. Jagodič, J. Kos, and D. Makovec. 2012. "Effect of Surface Charge on the Cellular Uptake of Fluorescent Magnetic Nanoparticles." *Journal of Nanoparticle Research* 14 (10): 1151. <https://doi.org/10.1007/s11051-012-1151-7>.
- Le Bras, A. 2022. "New Insights into the Origin of Amyloid Plaques." *Lab Animal* 51 (7): 187–187. <https://doi.org/10.1038/s41684-022-01007-x>.
- Lee, J.-H., D.-S. Yang, C. N. Goulbourne, E. Im, P. Stavrides, A. Pensalfini, H. Chan, et al. 2022. "Faulty Autolysosome Acidification in Alzheimer's Disease Mouse Models Induces Autophagic Build-up of A β in Neurons, Yielding Senile Plaques." *Nature Neuroscience* 25 (6): 688–701. <https://doi.org/10.1038/s41593-022-01084-8>.
- Leng, F., and P. Edison. 2021. "Neuroinflammation and Microglial Activation in Alzheimer Disease: Where Do We Go from Here?" *Nature Reviews Neurology* 17 (3): 157–172. <https://doi.org/10.1038/s41582-020-00435-y>.
- Liu, Y., M. Nguyen, A. Robert, and B. Meunier. 2019. "Metal Ions in Alzheimer's Disease: A Key Role or Not?" *Accounts of Chemical Research* 52 (7): 2026–2035. <https://doi.org/10.1021/acs.accounts.9b00248>.
- Livingston, G., J. Huntley, A. Sommerlad, D. Ames, C. Ballard, S. Banerjee, C. Brayne, et al. 2020. "Dementia Prevention, Intervention, and Care: 2020 Report of the Lancet Commission." *Lancet* 396 (10248): 413–446. [https://doi.org/10.1016/S0140-6736\(20\)30367-6](https://doi.org/10.1016/S0140-6736(20)30367-6).
- Lopez-Suarez, L., S. A. Awabdh, X. Coumoul, and C. Chauvet. 2022. "The SH-SY5Y Human Neuroblastoma Cell Line, a Relevant in Vitro Cell Model for Investigating Neurotoxicology in Human: Focus on Organic Pollutants." *Neurotoxicology* 92: 131–155. <https://doi.org/10.1016/j.neuro.2022.07.008>.
- Maher, B. A. 2019. "Airborne Magnetite- and Iron-Rich Pollution Nanoparticles: Potential Neurotoxicants and Environmental Risk Factors for Neurodegenerative Disease, Including Alzheimer's Disease." *Journal of Alzheimer's Disease* 71 (2): 361–375. <https://doi.org/10.3233/JAD-190204>.
- Maher, B. A., I. A. M. Ahmed, V. Karloukovski, D. A. MacLaren, P. G. Foulds, D. Allsop, D. M. A. Mann, R. Torres-Jardón, and L. Calderon-Garciduenas. 2016. "Magnetite Pollution Nanoparticles in the Human Brain." *Proceedings of the National Academy of Sciences* 113 (39): 10797–10801. <https://doi.org/10.1073/pnas.1605941113>.
- Mak, K., F. Yang, H. V. Vinters, S. A. Frautschy, and G. M. Cole. 1994. "Polyclonals to Beta-Amyloid(1-42) Identify Most Plaque and Vascular Deposits in Alzheimer Cortex, but Not Striatum." *Brain Research* 667 (1): 138–142. [https://doi.org/10.1016/0006-8993\(94\)91725-6](https://doi.org/10.1016/0006-8993(94)91725-6).
- Marciniak, E., A. Leboucher, E. Caron, T. Ahmed, A. Tailleux, J. Dumont, T. Issad, et al. 2017. "Tau Deletion Promotes Brain Insulin Resistance." *The Journal of Experimental Medicine* 214 (8): 2257–2269. <https://doi.org/10.1084/jem.20161731>.
- Martin, E.-R., J. Gandawijaya, and A. Oguro-Ando. 2022. "A Novel Method for Generating Glutamatergic SH-SY5Y Neuron-like Cells Utilizing B-27 Supplement." *Frontiers in Pharmacology* 13: 943627. <https://doi.org/10.3389/fphar.2022.943627>.
- Martorana, A., and G. Koch. 2014. "Is Dopamine Involved in Alzheimer's Disease?" *Frontiers in Aging Neuroscience* 6: 252. <https://doi.org/10.3389/fnagi.2014.00252>.
- Masters, C. L., R. Bateman, K. Blennow, C. C. Rowe, R. A. Sperling, and J. L. Cummings. 2015. "Alzheimer's Disease." *Nature Reviews Disease Primers* 1 (1): 15056. <https://doi.org/10.1038/nrdp.2015.56>.
- Mudher, A., M. Colin, S. Dujardin, M. Medina, I. Dewachter, S. M. Alavi Naini, E.-M. Mandelkow, et al. 2017. "What is the Evidence That Tau Pathology Spreads through Prion-like Propagation?" *Acta Neuropathologica Communications* 5 (1): 99. <https://doi.org/10.1186/s40478-017-0488-7>.
- Nemec, S., and S. Kralj. 2021. "A Versatile Interfacial Coassembly Method for Fabrication of Tunable Silica Shells with Radially Aligned Dual Mesopores on Diverse Magnetic Core Nanoparticles." *ACS Applied Materials & Interfaces* 13 (1): 1883–1894. <https://doi.org/10.1021/acsami.0c17863>.
- Nemec, S., S. Kralj, C. Wilhelm, A. Abou-Hassan, M.-P. Rols, and J. Kolosnjaj-Tabi. 2020. "Comparison of Iron Oxide

- Nanoparticles in Photothermia and Magnetic Hyperthermia: Effects of Clustering and Silica Encapsulation on Nanoparticles' Heating Yield." *Applied Sciences* 10 (20): 7322. <https://doi.org/10.3390/app10207322>.
- Nobili, A., E. C. Latagliata, M. T. Viscomi, V. Cavallucci, D. Cutuli, G. Giacobozzo, P. Krashia, et al. 2017. "Dopamine Neuronal Loss Contributes to Memory and Reward Dysfunction in a Model of Alzheimer's Disease." *Nature Communications* 8 (1): 14727. <https://doi.org/10.1038/ncomms14727>.
- Oakley, H., S. L. Cole, S. Logan, E. Maus, P. Shao, J. Craft, A. Guillozet-Bongaarts, et al. 2006. "Intraneuronal β -Amyloid Aggregates, Neurodegeneration, and Neuron Loss in Transgenic Mice with Five Familial Alzheimer's Disease Mutations: Potential Factors in Amyloid Plaque Formation." *The Journal of Neuroscience* 26 (40): 10129–10140. <https://doi.org/10.1523/JNEUROSCI.1202-06.2006>.
- Padmanabhan, P., A. Kneynsberg, E. Cruz, R. Amor, J.-B. Sibarita, and J. Götz. 2022. "Single-Molecule Imaging Reveals Tau Trapping at Nanometer-Sized Dynamic Hot Spots near the Plasma Membrane That Persists after Microtubule Perturbation and Cholesterol Depletion." *The EMBO Journal* 41 (19): e111265. <https://doi.org/10.15252/embj.2022111265>.
- Peebles, L. 2020. "How Air Pollution Threatens Brain Health." *Proceedings of the National Academy of Sciences* 117 (25): 13856–13860. <https://doi.org/10.1073/pnas.2008940117>.
- Pensalfini, A., R. Albay, S. Rasool, J. W. Wu, A. Hatami, H. Arai, L. Margol, et al. 2014. "Intracellular Amyloid and the Neuronal Origin of Alzheimer Neuritic Plaques." *Neurobiology of Disease* 71: 53–61. <https://doi.org/10.1016/j.nbd.2014.07.011>.
- Peters, R. J. B., A. G. Oomen, G. van Bommel, L. van Vliet, A. K. Undas, S. Munniks, R. L. A. W. Bleys, P. C. Tromp, W. Brand, and M. van der Lee. 2020. "Silicon Dioxide and Titanium Dioxide Particles Found in Human Tissues." *Nanotoxicology* 14 (3): 420–432. <https://doi.org/10.1080/17435390.2020.1718232>.
- Peters, R. J. B., G. van Bommel, Z. Herrera-Rivera, H. P. F. G. Helsper, H. J. P. Marvin, S. Weigel, P. C. Tromp, A. G. Oomen, A. G. Rietveld, and H. Bouwmeester. 2014. "Characterization of Titanium Dioxide Nanoparticles in Food Products: analytical Methods to Define Nanoparticles." *Journal of Agricultural and Food Chemistry* 62 (27): 6285–6293. <https://doi.org/10.1021/jf5011885>.
- Piller, C. 2023. "Report on Trial Death Stokes Alzheimer's Drug Fears." *Science* 380 (6641): 122–123. <https://doi.org/10.1126/science.adi2242>.
- Plascencia-Villa, G., A. Ponce, J. F. Collingwood, M. J. Arellano-Jiménez, X. Zhu, J. T. Rogers, I. Betancourt, M. José-Yacamán, and G. Perry. 2016. "High-Resolution Analytical Imaging and Electron Holography of Magnetite Particles in Amyloid Cores of Alzheimer's Disease." *Scientific Reports* 6 (1): 24873. <https://doi.org/10.1038/srep24873>.
- Popko, J., A. Fernandes, D. Brites, and L. M. Lanier. 2009. "Automated Analysis of NeuronJ Tracing Data." *Cytometry A* 75 (4): 371–376. <https://doi.org/10.1002/cyto.a.20660>.
- Riegerová, P., J. Břejcha, D. Bezděková, T. Chum, E. Mašínová, N. Čermáková, S. V. Ovsepian, M. Cebecauer, and M. Štefl. 2021. "Expression and Localization of A β PP in SH-SY5Y Cells Depends on Differentiation State." *Journal of Alzheimer's Disease* 82 (2): 485–491. <https://doi.org/10.3233/JAD-201409>.
- Rothmann, M. H., P. Møller, Y. J. Essig, L. Gren, V. B. Malmberg, M. Tunér, J. Pagels, A. M. Kraiss, and M. Roursgaard. 2023. "Genotoxicity by Rapeseed Methyl Ester and Hydrogenated Vegetable Oil Combustion Exhaust Products in Lung Epithelial (A549) Cells." *Mutagenesis* 38 (4): 238–249. <https://doi.org/10.1093/mutage/gead016>.
- Sala, A., S. P. Caminiti, L. Presotto, A. Pilotto, C. Liguori, A. Chiaravallotti, V. Garibotto, et al. 2021. "In Vivo Human Molecular Neuroimaging of Dopaminergic Vulnerability along the Alzheimer's Disease Phases." *Alzheimer's Research & Therapy* 13 (1): 187. <https://doi.org/10.1186/s13195-021-00925-1>.
- Scheltens, P., K. Blennow, M. M. B. Breteler, B. de Strooper, G. B. Frisoni, S. Salloway, and W. M. Van der Flier. 2016. "Alzheimer's Disease." *Lancet* 388 (10043): 505–517. [https://doi.org/10.1016/S0140-6736\(15\)01124-1](https://doi.org/10.1016/S0140-6736(15)01124-1).
- Schraufnagel, D. E. 2020. "The Health Effects of Ultrafine Particles." *Experimental & Molecular Medicine* 52 (3): 311–317. <https://doi.org/10.1038/s12276-020-0403-3>.
- Seo, S., M. Jang, H. Kim, J. H. Sung, N. Choi, K. Lee, and H. N. Kim. 2023. "Neuro-Glia-Vascular-on-a-Chip System to Assess Aggravated Neurodegeneration via Brain Endothelial Cells upon Exposure to Diesel Exhaust Particles." *Advanced Functional Materials* 33 (12): 2210123. <https://doi.org/10.1002/adfm.202210123>.
- Serrano-Pozo, A., M. L. Mielke, A. Muzitansky, T. Gómez-Isla, J. H. Growdon, B. J. Bacskai, R. A. Betensky, M. P. Frosch, and B. T. Hyman. 2012. "Stable Size Distribution of Amyloid Plaques over the Course of Alzheimer Disease." *Journal of Neuropathology and Experimental Neurology* 71 (8): 694–701. <https://doi.org/10.1097/NEN.0b013e31825e77de>.
- Sheikh, H. A., P. Y. Tung, E. Ringe, and R. J. Harrison. 2022. "Magnetic and Microscopic Investigation of Airborne Iron Oxide Nanoparticles in the London Underground." *Scientific Reports* 12 (1): 20298. <https://doi.org/10.1038/s41598-022-24679-4>.
- Shi, L., K. Steenland, H. Li, P. Liu, Y. Zhang, R. H. Lyles, W. J. Requia, et al. 2021. "A National Cohort Study (2000–2018) of Long-Term Air Pollution Exposure and Incident Dementia in Older Adults in the United States." *Nature Communications* 12 (1): 6754. <https://doi.org/10.1038/s41467-021-27049-2>.
- Shi, L., X. Wu, M. D. Yazdi, D. Braun, Y. A. Awad, Y. Wei, P. Liu, et al. 2020. "Long-Term Effects of PM_{2.5} on Neurological Disorders in the American Medicare Population: A Longitudinal Cohort Study." *The Lancet Planetary Health* 4 (12): e557–e565. [https://doi.org/10.1016/S2542-5196\(20\)30227-8](https://doi.org/10.1016/S2542-5196(20)30227-8).
- Song, B., J. Liu, X. Feng, L. Wei, and L. Shao. 2015. "A Review on Potential Neurotoxicity of Titanium Dioxide Nanoparticles." *Nanoscale Research Letters* 10 (1): 342. <https://doi.org/10.1186/s11671-015-1042-9>.
- Sotiropoulos, I., M.-C. Galas, J. M. Silva, E. Skoulakis, S. Wegmann, M. B. Maina, D. Blum, et al. 2017. "Atypical, Non-Standard Functions of the Microtubule Associated Tau Protein." *Acta Neuropathologica Communications* 5 (1): 91. <https://doi.org/10.1186/s40478-017-0489-6>.
- Suarez, A. E., and J. M. Ondov. 2002. "Ambient Aerosol Concentrations of Elements Resolved by Size and by Source: Contributions of Some Cytokine-Active Metals from Coal- and Oil-Fired Power Plants." *Energy & Fuels* 16 (3): 562–568. <https://doi.org/10.1021/ef010170c>.
- Suárez-Calvet, M., T. K. Karikari, N. J. Ashton, J. Lantero Rodríguez, M. Milà-Alomà, J. D. Gispert, G. Salvadó, et al.

2020. "Novel Tau Biomarkers Phosphorylated at T181, T217 or T231 Rise in the Initial Stages of the Preclinical Alzheimer's Continuum When Only Subtle Changes in A β Pathology Are Detected." *EMBO Molecular Medicine* 12 (12): e12921. <https://doi.org/10.15252/emmm.202012921>.
- Tadic, M., S. Kralj, M. Jagodic, D. Hanzel, and D. Makovec. 2014. "Magnetic Properties of Novel Superparamagnetic Iron Oxide Nanoclusters and Their Peculiarity under Annealing Treatment." *Applied Surface Science* 322: 255–264. <https://doi.org/10.1016/j.apsusc.2014.09.181>.
- Tahirbegi, B., A. J. Magness, M. E. Piersimoni, T. Knöpfel, K. R. Willison, D. R. Klug, and L. Ying. 2020. "A Novel A β 40 Assembly at Physiological Concentration." *Scientific Reports* 10 (1): 9477. <https://doi.org/10.1038/s41598-020-66373-3>.
- Takahashi, M., H. Miyata, F. Kametani, T. Nonaka, H. Akiyama, S. Hisanaga, and M. Hasegawa. 2015. "Extracellular Association of APP and Tau Fibrils Induces Intracellular Aggregate Formation of Tau." *Acta Neuropathologica* 129 (6): 895–907. <https://doi.org/10.1007/s00401-015-1415-2>.
- Titulaer, J., C. Björkholm, K. Feltmann, T. Malmlöf, D. Mishra, C. Bengtsson Gonzales, B. Schilström, and Å. Konradsson-Geuken. 2021. "The Importance of Ventral Hippocampal Dopamine and Norepinephrine in Recognition Memory." *Frontiers in Behavioral Neuroscience* 15: 667244. <https://doi.org/10.3389/fnbeh.2021.667244>.
- Umek, P., R. C. Korosec, B. Jancar, R. Dominko, and D. Arcon. 2007. "The Influence of the Reaction Temperature on the Morphology of Sodium Titanate 1D Nanostructures and Their Thermal Stability." *Journal of Nanoscience and Nanotechnology* 7 (10): 3502–3508. <https://doi.org/10.1166/jnn.2007.838>.
- Underwood, E. 2017. "The Polluted Brain." *Science* 355 (6323): 342–345. <https://doi.org/10.1126/science.355.6323.342>.
- Urbančič, I., M. Garvas, B. Kokot, H. Majaron, P. Umek, H. Cassidy, M. Škarabot, et al. 2018. "Nanoparticles Can Wrap Epithelial Cell Membranes and Relocate Them across the Epithelial Cell Layer." *Nano Letters* 18 (8): 5294–5305. <https://doi.org/10.1021/acs.nanolett.8b02291>.
- Viskup, R., C. Wolf, and W. Baumgartner. 2020. *Major Chemical Elements in Soot and Particulate Matter Exhaust Emissions Generated from in-Use Diesel Engine Passenger Vehicles*. London, UK: IntechOpen Limited. <https://doi.org/10.5772/intechopen.90452>.
- Walker, L. C. 2020. "A β Plaques." *Free Neuropathology* 1: 31. <https://doi.org/10.17879/freeneuropathology-2020-3025>.
- Weichenthal, S., L. Pinault, T. Christidis, R. T. Burnett, J. R. Brook, Y. Chu, D. L. Crouse, et al. 2022. "How Low Can You Go? Air Pollution Affects Mortality at Very Low Levels." *Science Advances* 8 (39): eabo3381. <https://doi.org/10.1126/sciadv.abo3381>.
- Wilson, D. M., M. R. Cookson, L. Van Den Bosch, H. Zetterberg, D. M. Holtzman, and I. Dewachter. 2023. "Hallmarks of Neurodegenerative Diseases." *Cell* 186 (4): 693–714. <https://doi.org/10.1016/j.cell.2022.12.032>.
- Xie, H., L. Hu, and G. Li. 2010. "SH-SY5Y Human Neuroblastoma Cell Line: In Vitro Cell Model of Dopaminergic Neurons in Parkinson's Disease." *Chinese Medical Journal* 123 (8): 1086–1092.
- Xiong, F., W. Ge, and C. Ma. 2019. "Quantitative Proteomics Reveals Distinct Composition of Amyloid Plaques in Alzheimer's Disease." *Alzheimer's & Dementia* 15 (3): 429–440. <https://doi.org/10.1016/j.jalz.2018.10.006>.
- Younan, D., A. J. Petkus, K. F. Widaman, X. Wang, R. Casanova, M. A. Espeland, M. Gatz, et al. 2020. "Particulate Matter and Episodic Memory Decline Mediated by Early Neuroanatomic Biomarkers of Alzheimer's Disease." *Brain: a Journal of Neurology* 143 (1): 289–302. <https://doi.org/10.1093/brain/awz348>.
- Ze, Y., L. Sheng, X. Zhao, J. Hong, X. Ze, X. Yu, X. Pan, et al. 2014. "TiO₂ Nanoparticles Induced Hippocampal Neuroinflammation in Mice." *PLOS One* 9 (3): e92230. <https://doi.org/10.1371/journal.pone.0092230>.
- Zhang, H., D. Yu, S. Liu, C. Liu, Z. Liu, J. Ren, and X. Qu. 2022. "NIR-II Hydrogen-Bonded Organic Frameworks (HOFs) Used for Target-Specific Amyloid- β Photo-oxygenation in an Alzheimer's Disease Model." *Angewandte Chemie* 61 (2): e202109068. <https://doi.org/10.1002/anie.202109068>.
- Zhang, H., Y. Cao, L. Ma, Y. Wei, and H. Li. 2021. "Possible Mechanisms of Tau Spread and Toxicity in Alzheimer's Disease." *Frontiers in Cell and Developmental Biology* 9: 707268. <https://doi.org/10.3389/fcell.2021.707268>.
- Zhang, X., X. Chen, and X. Zhang. 2018. "The Impact of Exposure to Air Pollution on Cognitive Performance." *Proceedings of the National Academy of Sciences* 115 (37): 9193–9197. <https://doi.org/10.1073/pnas.1809474115>.